Supporting Information

Two-Dimensional Mesoporous Carbon Doped with Fe-N Active Sites for Efficient Oxygen Reduction

Yifan Ye,[†,‡] Haobo Li,[†,‡] Fan Cai,[†,‡] Chengcheng Yan,[†,‡] Rui Si,[§] Shu Miao,[†] Yanshuo Li,*[,‖] Guoxiong Wang,*[,†] and Xinhe Bao[†]

[†]State Key Laboratory of Catalysis, CAS Center for Excellence in Nanoscience, Dalian National Laboratory for Clean Energy, Dalian Institute of Chemical Physics, Chinese Academy of Sciences, Dalian 116023, China

[‡] University of Chinese Academy of Sciences, Beijing 100039, China

[§]Shanghai Synchrotron Radiation Facility, Shanghai Institute of Applied Physics, Chinese Academy of Sciences, Shanghai 201204, China

[‖]School of Material Science and Chemical Engineering, Ningbo University, Ningbo 315211, China

E-mail addresses: liyanshuo@nbu.edu.cn, wanggx@dicp.ac.cn.

Figure S1. Doping energy of Fe atom into Zn atom sites of ZIF-7 framework, with the schematic diagram of the corresponding atomic structures. The energies of Fe and Zn atoms are in reference to their citrate complexes (ferric citrate and zinc citrate).

Figure S2. Doping energy of Fe atom into Zn atom sites of ZIF-7 framework, with the schematic diagram of the corresponding atomic structures.

Figure S3. (a) SEM and (b) HRSEM images of ZIF-(12, 8h).

Figure S4. (a) SEM and (b) HRSEM images of ZIF-(12, 16h).

Figure S5. SEM images of Fe©N-C-12.

Figure S6. High-resolution HADDF-STEM images of Fe©N-C-12.

Figure S7. Nitrogen adsorption–desorption isotherms of ZIF-7 derived catalysts with different AFC dosages after impregnation for 24 h.

Figure S8. Electron transfer number and HO_2^- selectivity of ZIF-7 derived catalysts with different impregnation durations.

Figure S9. Raman spectra of ZIF-7 derived catalysts with different impregnation durations.

Figure S10 XRD patterns of ZIF-L, ZIF-(12, 24h), ZIF-(30, 24h) and ZIF-(60, 24h).

Figure S11. LSV curves of Fe©N-C-12 in O_2-saturated 0.1 M KOH solution at different rotation rates.

Figure S12. (a) The schematic diagram and (b) photograph of in situ XAS cell in working condition for ORR; (c-d) In situ XANES and EXAFS of Fe©N-C-12 under ORR test with different potentials.

Table S1. Fe content (wt%) of ZIF-7 derived catalysts with different impregnation durations as confirmed by ICP-OES.

Table S2. Porosity characters of ZIF-7 derived catalysts with different impregnation durations.

Table S3. Porosity characters of ZIF-7 derived catalysts with different AFC dosages.

Table S4. Fe content (wt%) of ZIF-7 derived catalysts with different AFC usages as confirmed by ICP-OES.

Table S5. Mass activities of different single-atom non-precious-metal catalysts in O_2-saturated 0.1 M KOH solution (1600 rpm)

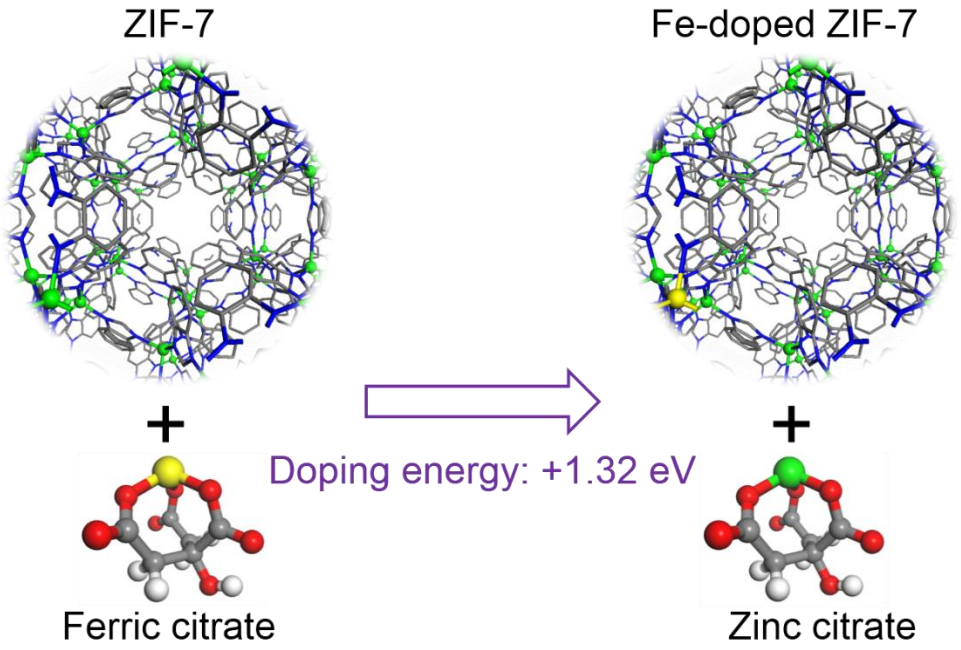

Figure S1. Doping energy of Fe atom into Zn atom sites of ZIF-7 framework, with the schematic diagram of the corresponding atomic structures. The energies of Fe and Zn atoms are in reference to their citrate complexes (ferric citrate and zinc citrate).

C: grey; N: blue; Zn: green; H: white; O: red; Fe: yellow.

The doping energy is calculated by: $\Delta E_{doping} = E_{total} – [E(ZIF\text{-}7) – E(Zn\text{-}citrate) + E(Fe\text{-}citrate)]$ where E_{total} is the energy of Fe-doped ZIF-7, E(ZIF-7) is the energy of perfect ZIF-7, E(Zn-citrate) and E(Fe-citrate) are the energies of ferric citrate and zinc citrate complexes, respectively.

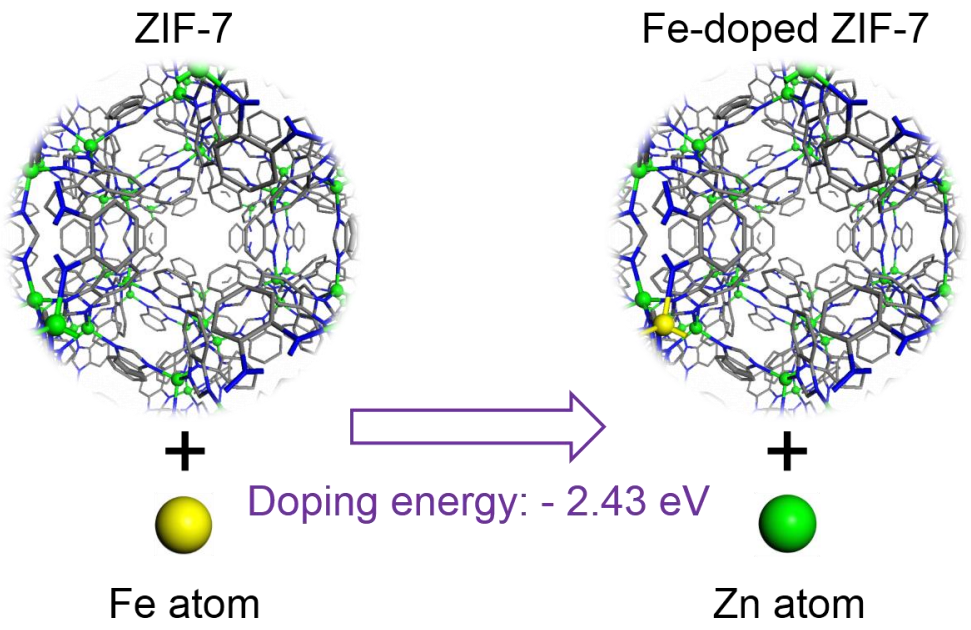

Figure S2. Doping energy of Fe atom into Zn atom sites of ZIF-7 framework, with the schematic diagram of the corresponding atomic structures. C: grey; N: blue; Zn: green; Fe: yellow.

The doping energy is calculated by: $\Delta E_{doping} = E_{total} - [E(ZIF\text{-}7) - E(Zn\text{-}atom) + E(Fe\text{-}atom)]$ where E_{total} is the energy of Fe-doped ZIF-7, E(ZIF-7) is the energy of perfect ZIF-7, E(Zn-atom) and E(Fe-atom) are the energies of single Fe atom and Zn atom, respectively.

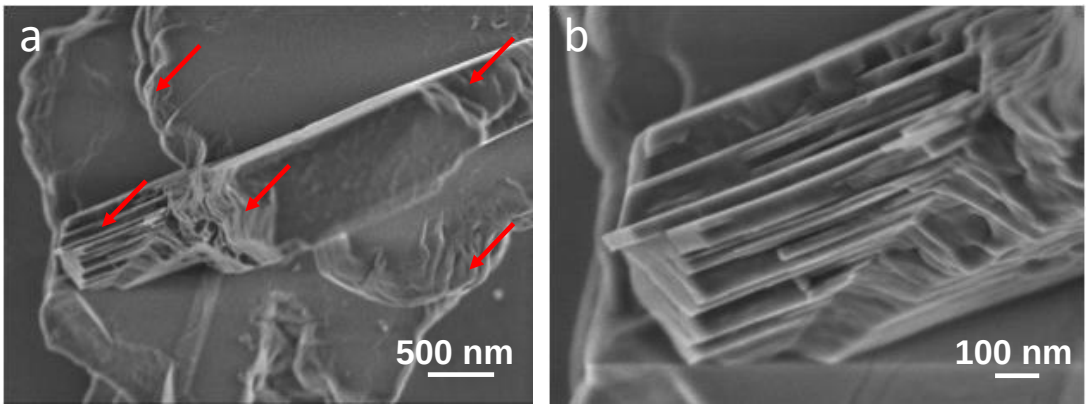

Figure S3. (a) SEM and (b) HRSEM images of ZIF-(12, 8h). The red arrows in Figure S3a show the self-assembly of 2D ZIF structure in the partially-transformed ZIF-(12, 8h).

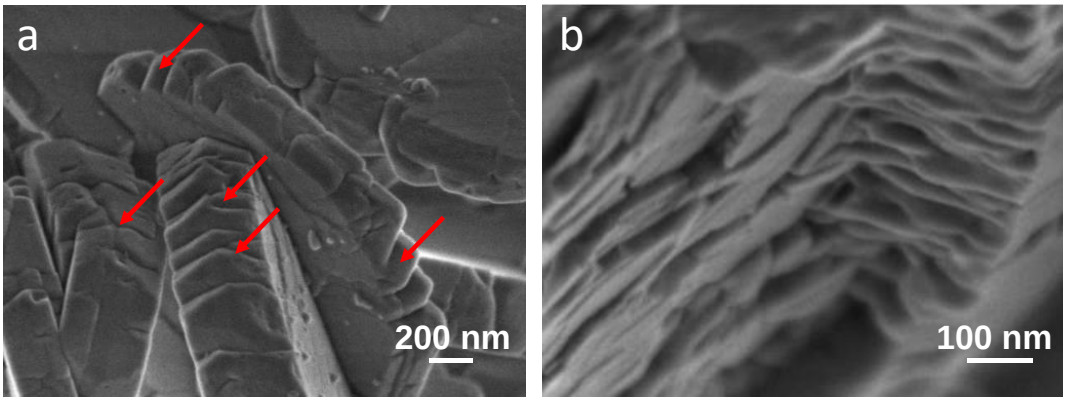

Figure S4. (a) SEM and (b) HRSEM images of ZIF-(12, 16h). The red arrows in Figure S4a show the self-assembly of 2D ZIF structure in the partially-transformed ZIF-(12, 16h).

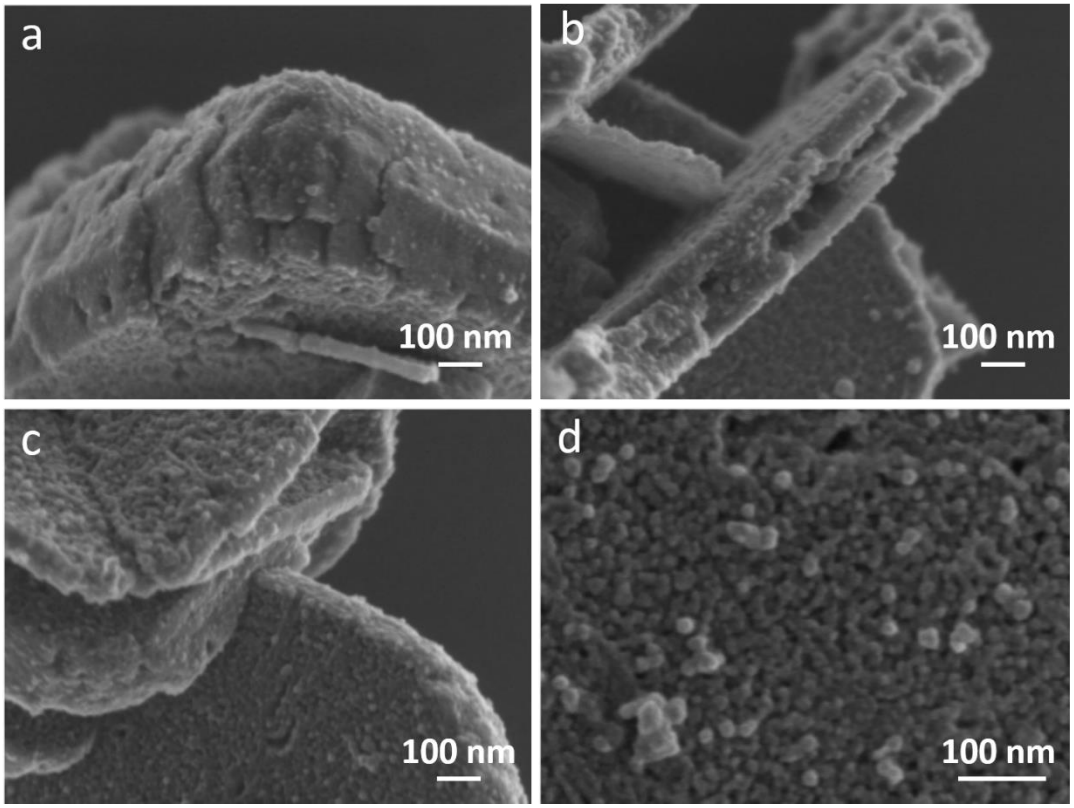

Figure S5. SEM images of Fe©N-C-12.

The SEM images of Fe©N-C-12 obviously show the highly porous structure with interconnected pores throughout the micrometer-length nanosheet.

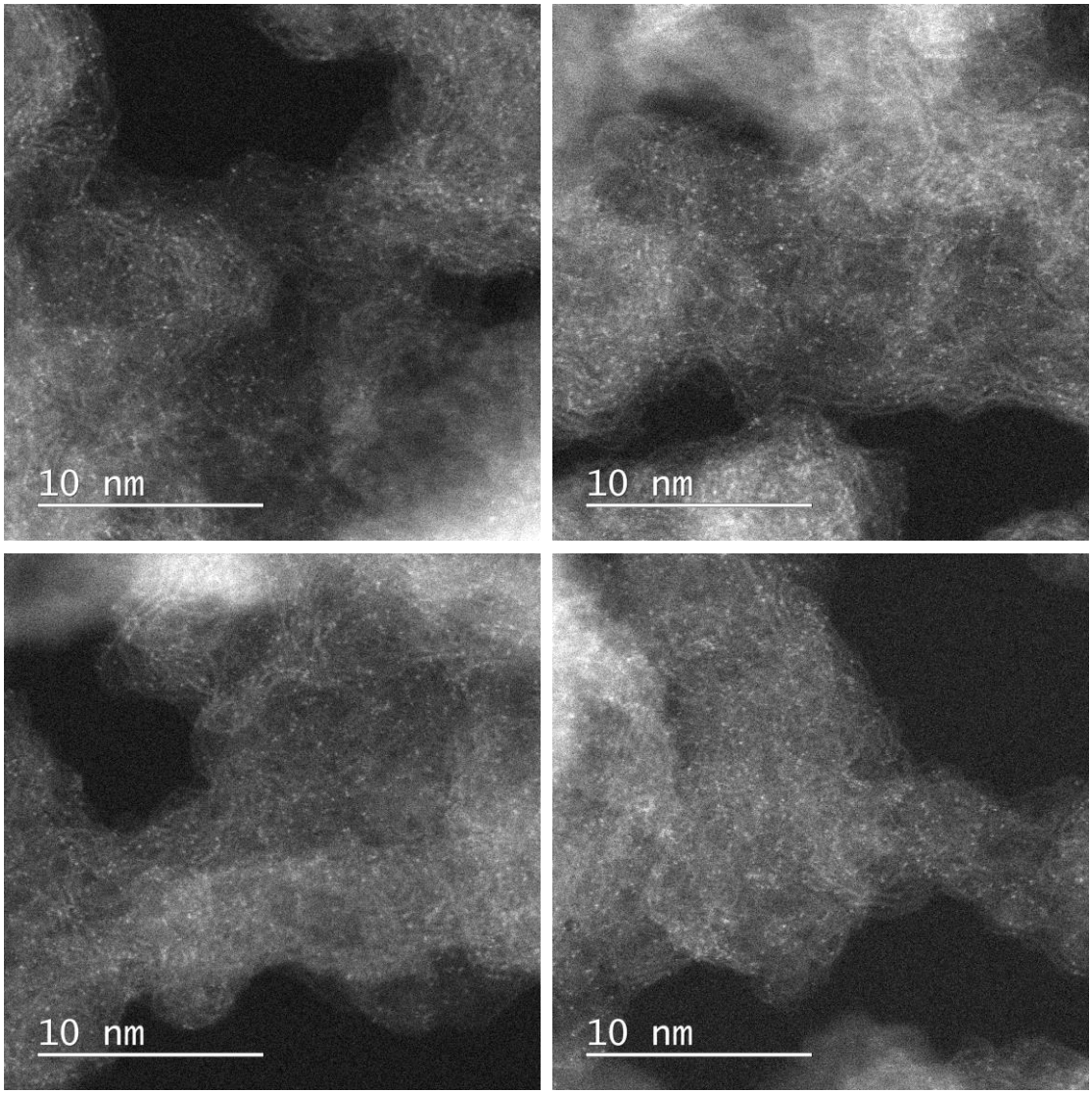

Figure S6. High-resolution HADDF-STEM images of Fe©N-C-12.

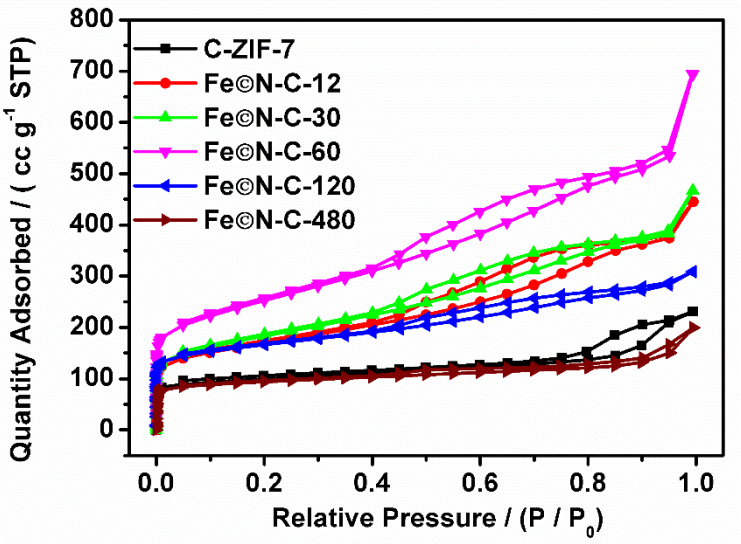

Figure S7. Nitrogen adsorption–desorption isotherms of ZIF-7 derived catalysts with different AFC dosages after impregnation for 24 h.

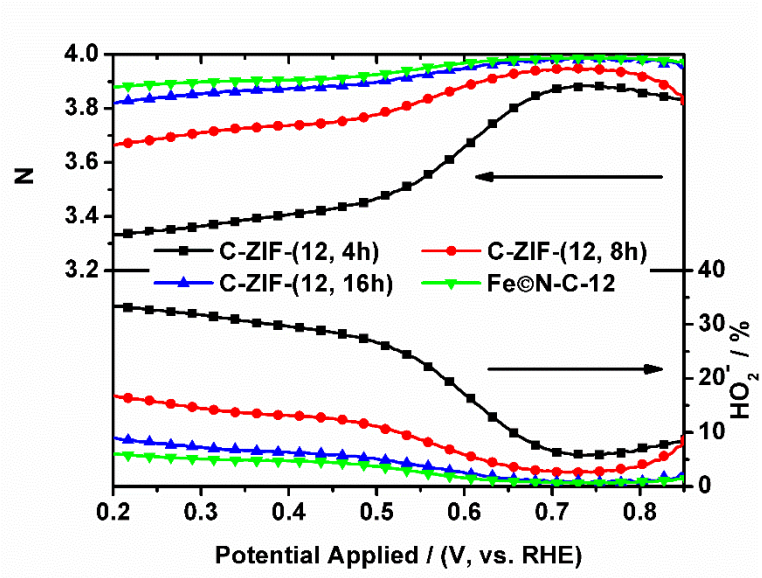

Figure S8. Electron transfer number and HO_2^- selectivity of ZIF-derived catalysts with different impregnation durations; Catalyst usages were all kept 61 μg.

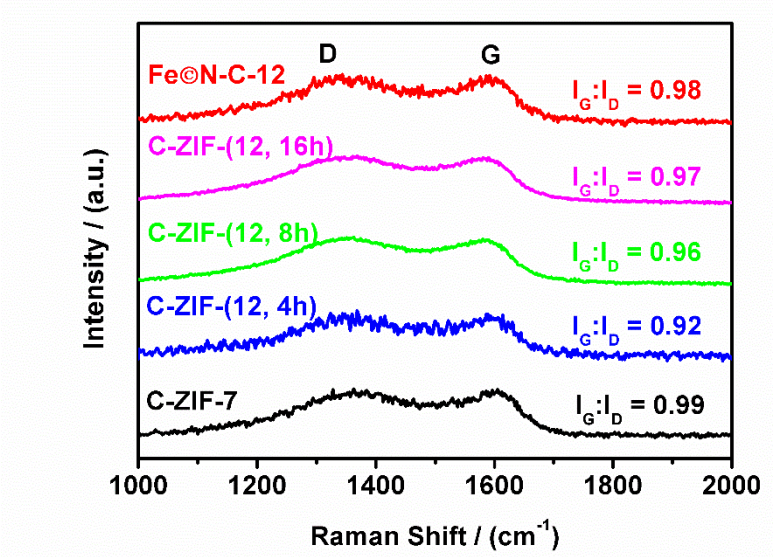

Figure S9. Raman spectra of ZIF-7 derived catalysts with different impregnation durations.

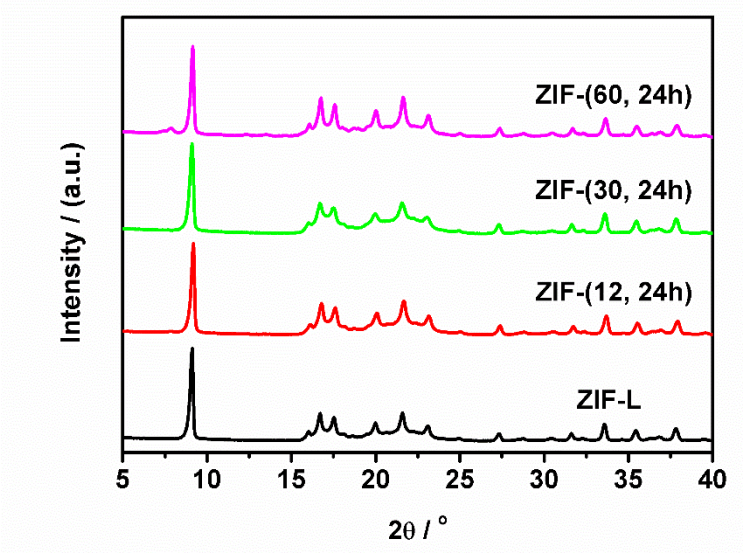

Figure S10 XRD patterns of ZIF-L, ZIF-(12, 24h), ZIF-(30, 24h) and ZIF-(60, 24h).

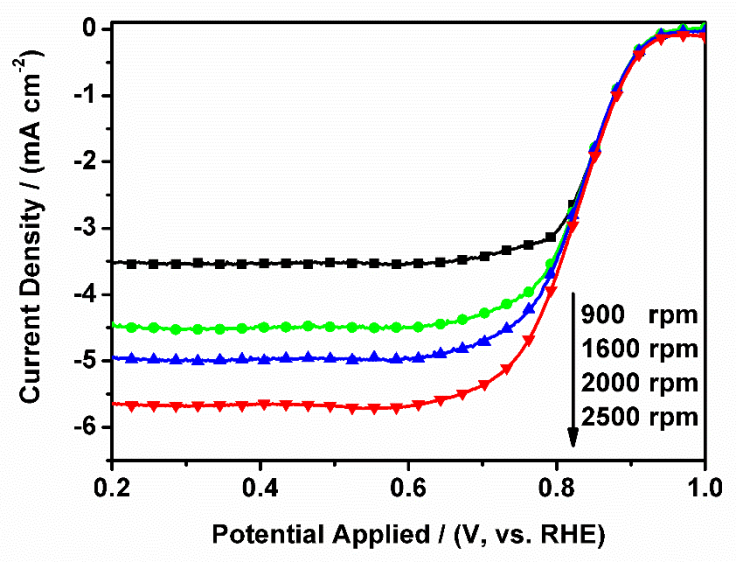

Figure S11. LSV curves of Fe©N-C-12 in O_2-saturated 0.1 M KOH solution at different rotation rates.

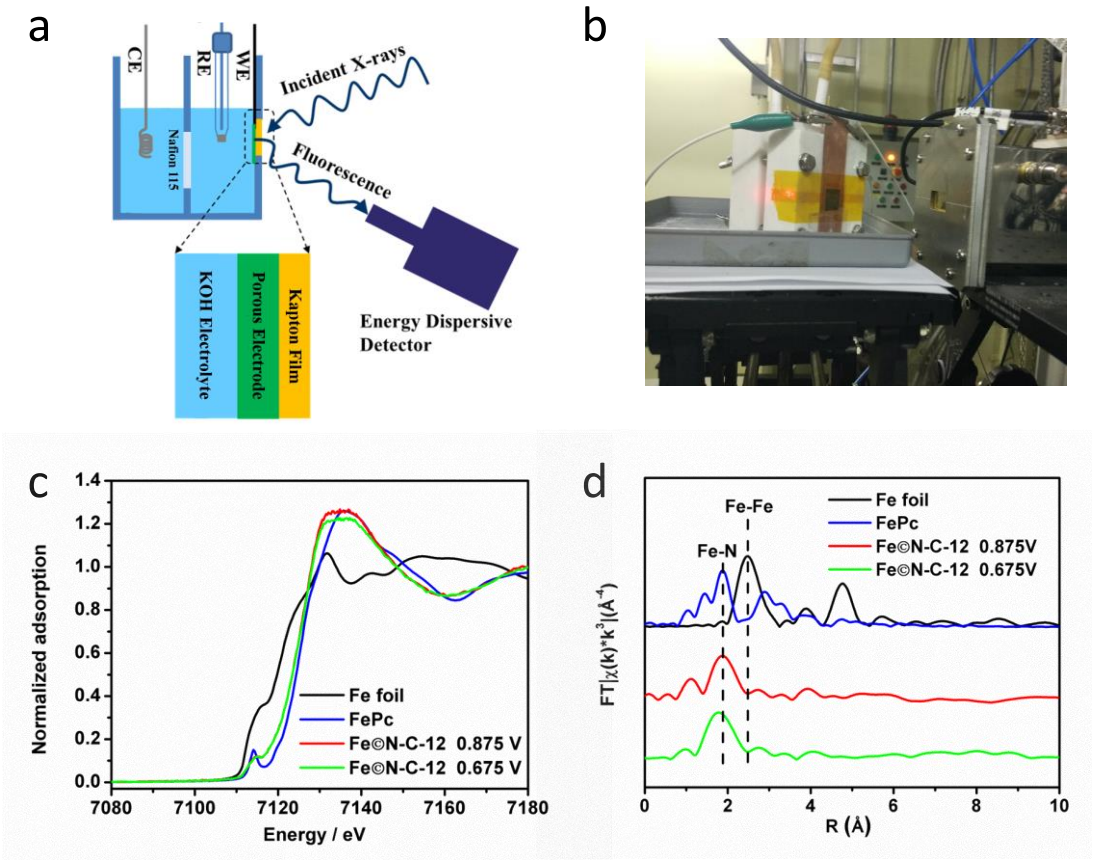

Figure S12. (a) The schematic diagram and (b) photograph of In situ XAS cell in working condition for ORR; (c-d) In situ XANES and EXAFS of Fe©N-C-12 under ORR test with different potentials (V, vs. RHE), R(Å), distance in angstroms. k, wavenumber. All the data was obtained in O_2-saturated 0.1 M KOH solution.

Table S1. Fe content (wt%) of ZIF-7 derived catalysts with different impregnation durations as confirmed by ICP-OES.

Samples	Before pyrolysis	After pyrolysis & acid leaching
	Fe (wt%)	Fe (wt%)
ZIF-7	—	—
ZIF-(12, 4h)	0.21	0.40
ZIF-(12, 8h)	0.20	0.37
ZIF-(12, 16h)	0.19	0.38
ZIF-(12, 24h)	0.22	0.37

Table S2. Porosity characters of ZIF-7 derived catalysts with different impregnation durations.

Catalyst	BET surface area ($m^2 g^{-1}$)	Micropore surface area ($m^2 g^{-1}$)	External surface area ($m^2 g^{-1}$)	V_{total} ($cc\ g^{-1}$)[a]	V_{μ} ($cc\ g^{-1}$)[b]	ΔV ($cc\ g^{-1}$)[c]
C-ZIF-7	356.9	226.1	130.8	0.357	0.097	0.260
C-ZIF-(12, 4h)	384.1	116.1	268.0	0.452	0.054	0.398
C-ZIF-(12, 8h)	499.0	137.3	361.7	0.618	0.064	0.554
C-ZIF-(12, 16h)	610.5	121.2	489.3	0.793	0.058	0.735
Fe©N-C-12	594.5	192.5	402.0	0.691	0.089	0.602

[a] Total pore volume was calculated at P/P_0=0.995;

[b] Micropore volume was calculated using t-plot method.

[c] ΔV means the difference between V_{total} and V_{μ}.

Table S3. Porosity characters of ZIF-7 derived catalysts with different AFC dosages.

Catalyst	BET surface area ($m^2 g^{-1}$)	Micropore surface area ($m^2 g^{-1}$)	External surface area ($m^2 g^{-1}$)	V_{total} (cc g^{-1})[a]	V_{μ} (cc g^{-1})[b]	ΔV (cc g^{-1})[c]
C-ZIF-7	356.9	226.1	130.8	0.357	0.097	0.260
Fe©N-C-12	594.5	192.5	402.0	0.691	0.089	0.602
Fe©N-C-30	644.2	170.9	473.3	0.722	0.078	0.644
Fe©N-C-60	888.9	227.3	661.6	1.073	0.105	0.968
Fe©N-C-120	594.8	323.5	271.3	0.479	0.141	0.338
Fe©N-C-480	346.5	247.2	99.3	0.309	0.103	0.206

[a] Total pore volume was calculated at P/P_0=0.995;

[b] Micropore volume was calculated using t-plot method.

[c] ΔV means the difference between V_{total} and V_{μ}.

Table S4. Fe content (wt%) of ZIF-7 derived catalysts with different AFC usages as confirmed by ICP-OES.

Samples	Before pyrolysis Fe (wt%)	After pyrolysis & acid leaching Fe (wt%)
ZIF-7	—	—
ZIF-(12, 24h)	0.22	0.37
ZIF-(30, 24h)	0.37	0.69
ZIF-(60, 24h)	0.42	0.87
ZIF-(120, 24h)	0.47	0.82
ZIF-(480, 24h)	1.13	2.38

Table S5. Mass activities of different single-atom non-precious-metal catalysts in O_2-saturated 0.1 M KOH solution (1600 rpm).

Catalyst	metal loading (μg_{metal} cm^{-2})	Activity @ 0.80V (mA μg_{metal}^{-1})	References
Fe©N-C-12	1.15	2.92	This work
Co SAs/N-C(900)	17.54	0.33	1
Fe-ISAs/CN	8.81	0.64	2
S,N-Fe/N/C-CNT	20.00	0.24	3
SA-Fe-NHPC	2.30	1.67	4
CNT/PC	23.20	0.23	5
Fe-N/C-700	3.21	1.48	6
FeN_2/NOMC-3	7.53	0.59	7
Fe-N_x/HPC	1.55	2.58	8
Fe,N/PGC-30	6.22	0.58	9

References

1. Yin, P.; Yao, T.; Wu, Y.; Zheng, L.; Lin, Y.; Liu, W.; Ju, H.; Zhu, J.; Hong, X.; Deng, Z.; Zhou, G.; Wei, S.; Li, Y. *Angew. Chem. Int. Ed.* **2016,** *55*, 10800-10805.
2. Chen, Y.; Ji, S.; Wang, Y.; Dong, J.; Chen, W.; Li, Z.; Shen, R.; Zheng, L.; Zhuang, Z.; Wang, D.; Li, Y. *Angew. Chem. Int. Ed.* **2017,** *56*, 6937-6941.
3. Chen, P.; Zhou, T.; Xing, L.; Xu, K.; Tong, Y.; Xie, H.; Zhang, L.; Yan, W.; Chu, W.; Wu, C.; Xie, Y. *Angew. Chem. Int. Ed.* **2017,** *56*, 610-614.
4. Zhang, Z.; Gao, X.; Dou, M.; Ji, J.; Wang, F. *Small* **2017,** *1*, 1004-1009.
5. Sa, Y. J.; Seo, D.-J.; Woo, J.; Lim, J. T.; Cheon, J. Y.; Yang, S. Y.; Lee, J. M.; Kang, D.; Shin, T. J.; Shin, H. S.; Jeong, H. Y.; Kim, C. S.; Kim, M. G.; Kim, T.-Y.; Joo, S. H. *J. Am. Chem. Soc.* **2016,** *138*, 15046-15056.
6. Yang, Z. K.; Lin, L.; Xu, A.-W. *Small* **2016,** *12*, 5710-5719.

7. Shen, H.; Gracia-Espino, E.; Ma, J.; Tang, H.; Mamat, X.; Wagberg, T.; Hu, G.; Guo, S. *Nano Energy* **2017,** *35*, 9-16.
8. Zhang, Z.; Gao, X.; Dou, M.; Ji, J.; Wang, F. *J. Mater. Chem. A* **2017,** *5*, 1526-1532.
9. Gu, W.; Hu, L.; Li, J.; Wang, E. *J. Mater. Chem. A* **2016,** *4*, 14364-14370.